Proc. Natl. Acad. Sci. USA
Vol. 95, pp. 5807–5811, May 1998
Neurobiology

Morphine disrupts long-range synchrony of gamma oscillations in hippocampal slices

(hippocampus/interneuron/μ-opioid)

M. A. WHITTINGTON*†, R. D. TRAUB‡, H. J. FAULKNER*, J. G. R. JEFFERYS‡, AND K. CHETTIAR*

*Cellular and Integrative Biology Section, Biomedical Sciences Division, Imperial College School of Medicine, London, W2 1PG, and ‡Department of Physiology, The Medical School, University of Birmingham, Birmingham, B15 2TT, U.K.

Edited by Rodolfo R. Llinás, New York University Medical Center, New York, NY, and approved March 8, 1998 (received for review December 16, 1997)

ABSTRACT **Oscillations in neuronal population activity within the gamma frequency band (>25 Hz) have been correlated with cognition: Gamma oscillations could bind together features of a sensory stimulus by generating synchrony between discrete cortical areas [Eckhorn, R., Bauer, R., Jordan, W., Brosch, M., Kruse, W., Munk, M. & Reitboeck, H. J. (1989) *Biol. Cybern.* 60, 121–130; Singer, W. & Gray, C. M. (1995) *Annu. Rev. Neurosci.* 18, 555–556]. Herein we demonstrate that morphine and β-endorphin disrupt this long-range synchrony of gamma oscillations while leaving the synchrony of local oscillations relatively intact. The effect is caused by a decrease in type A γ-aminobutyric acid receptor-mediated inhibition of both excitatory pyramidal cells and inhibitory interneurons. The effects of morphine on gamma oscillations were blocked by μ-opioid receptor antagonists but not by antagonists of δ or κ receptors. Morphine also produced burst firing in interneurons, because synaptic excitation from pyramidal cells was no longer balanced by synchronous inhibitory postsynaptic potentials. The loss of synchrony of gamma oscillations induced by morphine may constitute one mechanism involved in producing the cognitive deficits that this drug causes clinically.**

Clinically, morphine administration produces analgesia, amnesia, euphoria, and mental clouding. At higher doses, morphine can act as a general anesthetic. Cognitive impairment typically takes the form of a poor performance in objective tests for attention, name–face recognition, and visuospatial coding tasks (1). In the central nervous system, the major effects of morphine are generated via its action as a partial agonist at μ-opioid receptors (2, 3). These receptors are found throughout the central nervous system, particularly in the limbic system (4). In the hippocampus μ-opioid receptors are mainly localized in area CA1 (5), though neuronal responses to activation of these receptors have been reported in area CA3 (6) and the dentate gyrus (5). The presence of endogenous ligands for the morphine-sensitive μ-opioid receptor has been well documented (see ref. 7) with high affinity and efficacy reported for β-endorphin, endomorphins, dynorphin A, and Met- and Leu-enkephalin.

The primary effect of μ receptor activation appears to be a potentiation of the excitability of principal cells in the archicortex by a disinhibitory mechanism (8). These authors reported a marked diminution of evoked type A γ-aminobutyric acid ($GABA_A$) receptor-mediated inhibitory postsynaptic potentials (IPSPs) in both hippocampal principal cells and interneurons. Further work has shown that μ-opioid receptor activation decreases the presynaptic release of GABA by a G protein-mediated mechanism (6). The activity of, and consequent GABA release from, inhibitory interneurons in the hippocampus and neocortex has been shown to affect critically the ability of the central nervous system to generate and maintain fast oscillations within the EEG gamma band (>25 Hz) *in vitro* and *in vivo* (9–11). The magnitude and kinetics of $GABA_A$-receptor-mediated inhibitory postsynaptic events in interneurons appear to be particularly important (10, 12). Gamma oscillations in interneuron networks are able to entrain principal cell activity. They can mediate synchronous firing patterns in spatially separate areas of archicortex when pyramidal cells excite interneurons strongly enough (13).

The process of synchronizing outputs from different areas of cortex appears to play a role in certain forms of cognitive processing (14–16), in particular the response to novel sensory stimuli. In the hippocampus gamma oscillations are particularly prevalent during theta activity and immediately after sharp waves in the awake behaving rat (10, 17, 18). We studied the effects of morphine on an *in vitro* hippocampal model of this long-range synchrony of gamma oscillations and demonstrate a disruption of interareal communication at concentrations relevant to those reported clinically during morphine-induced cognitive impairment.

METHODS

Experimental Methods. Transverse, 400- to 450-μm-thick dorsal hippocampal slices were prepared from brains of male Sprague–Dawley rats, 250–350 g. Brief tetanic stimuli (100 Hz, 100–200 ms, and 8–25 V) were delivered simultaneously to the stratum oriens at two recording sites (area CA1a and CA1c, separation 1.5–2.5 mm, Fig. 1*a*). Field potentials were recorded at the level of stratum pyramidale at each site simultaneously. Data were taken from five slices with a minimum of three replicates per slice per drug concentration. Frequency and phase relationships for field potential oscillations were measured by performing auto- and cross-correlation analyses of the posttetanic oscillations (200-ms time window starting at the beginning of the oscillation).

$GABA_A$-receptor-mediated postsynaptic events in CA1 pyramidal cells (IPSCs) were isolated from ionotropic glutamatergic excitation by the bath application of 3-[(*R*)-2-carboxypiperazin-4-yl]propyl-1-phosphonic acid at 50 μM and 6-nitro-7-sulfamoylbenzo[*f*]quinoxaline-2,3-dione

The publication costs of this article were defrayed in part by page charge payment. This article must therefore be hereby marked "*advertisement*" in accordance with 18 U.S.C. §1734 solely to indicate this fact.

This paper was submitted directly (Track II) to the *Proceedings* office. Abbreviations: $GABA_A$ receptor; type A γ-aminobutyric acid receptor; IPSP, inhibitory postsynaptic potential; IPSC, inhibitory postsynaptic current; NBQX, 6-nitro-7-sulfamoylbenzo[*f*]quinoxaline-2,3-dione; AMPA, α-amino-3-hydroxy-5-methyl-4-isoxazolepropionic acid.

†To whom reprint requests should be addressed at: Department of Physiology and Biophysics, Imperial College School of Medicine at St. Mary's, The Medical School, Norfolk Place, London W2 1PG, U.K. e-mail: m.whittington@sm.ic.ac.uk.

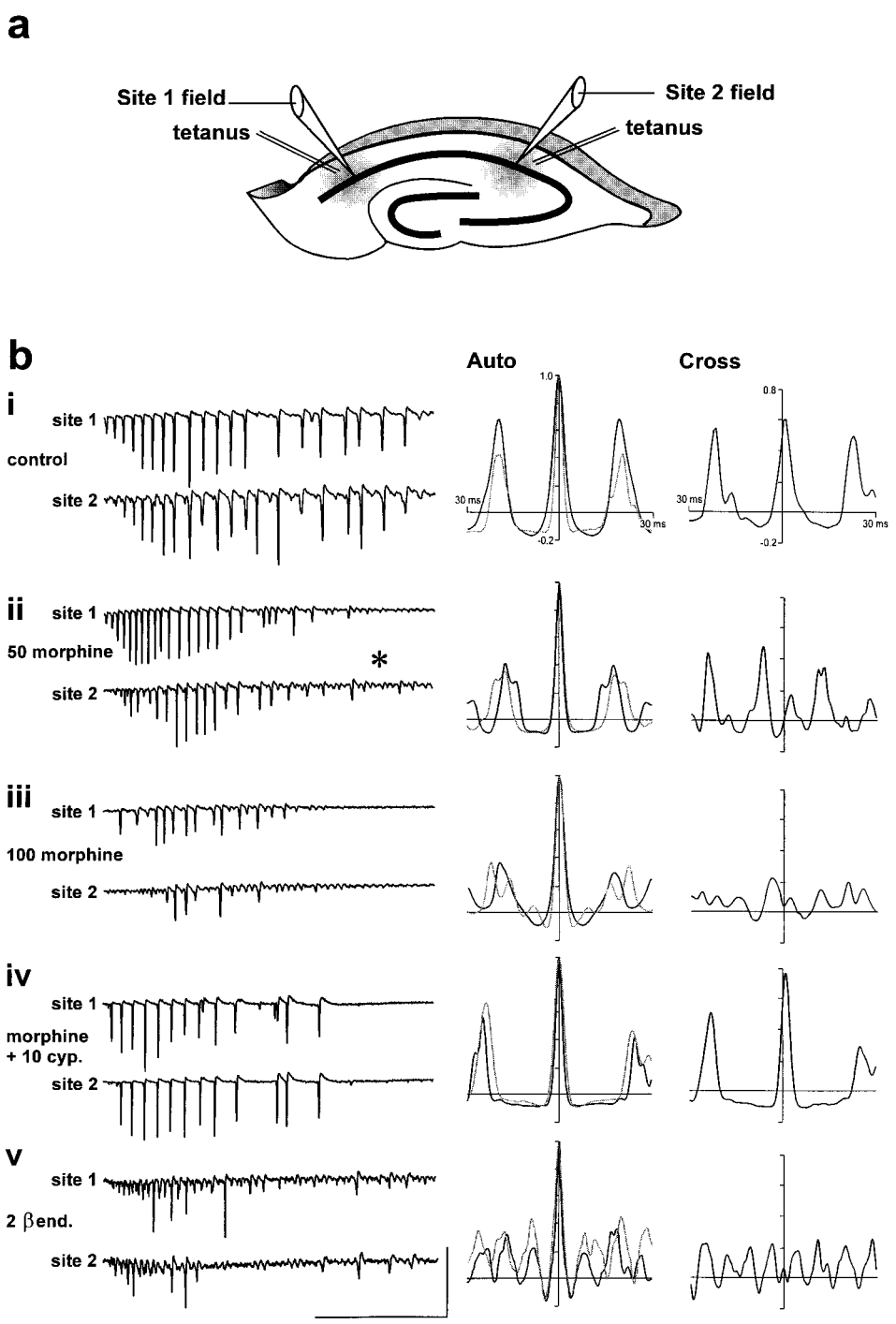

FIG. 1. μ-Opioid receptor activation disrupts gamma oscillations and long-range synchrony. (*a*) Schematic of a hippocampal slice illustrating the sites of stimulation/recording in area CA1. (*b*) Posttetanic gamma oscillations evoked simultaneously at two sites demonstrate rhythmicity (frequency = 52 ± 2 Hz, $n = 6$, from autocorrelograms) and synchrony (phase lag/lead = 1.0 ± 0.6 ms, $n = 6$, from cross-correlograms) in control slices (*bi*). Morphine, added to the slice bathing medium, causes a concentration-dependent disruption of rhythmicity with multiple autocorrelation peaks seen at concentrations above 20 μM. Synchrony between sites is also detrimentally affected at these concentrations with a significant increase in phase lag to 4.6 ± 0.7 ms at 50 μM ($P < 0.05$) (*bii* and *biii*). Bath application of 10–20 μM cyprodime (a selective μ-receptor antagonist) reversed the effects of 50–100 μM morphine on rhythmicity and synchrony (*biv*). The above effects of morphine were mimicked by 2 μM β-endorphin (*bv*). Scale bars equal 5 mV and 300 ms.

(NBQX) at 50 μM to the artificial cerebrospinal fluid (aCSF). 2-Hydroxysaclofen at 0.2 mM was also added to block $GABA_B$-receptor-mediated inhibition. IPSCs were recorded by using a discontinuous single-electrode voltage clamp via microelectrodes, with a resistance of 30–60 MΩ, filled with 2 M potassium methylsulfate/50 mM lidocaine *N*-ethyl bromide (QX314). Mean cell membrane resistance was 58 ± 12 MΩ (in the presence of QX314), and resting potential was −68 ± 4 mV. Trains of IPSCs were evoked by pressure ejection (0.8–1.2 kg/cm^2, 2 ms), of 10 mM L-glutamate at the surface of the hippocampal slice in the perisomatic region. All currents were recorded with a holding potential of −40 mV (14). Intracellular recordings of oscillatory activity in pyramidal cells ($n = 48$) and physiologically identified inhibitory interneurons ($n = 9$) were also made in bridge mode with glass microelectrodes filled with 2 M potassium methylsulfate or potassium acetate (30–80 MΩ).

Simulation Methods. A distributed network model of the CA1 region was constructed by using an approach similar to that described in ref. 19, using component pyramidal cell and interneuron models as in refs. 20 and 21. Differences from the previous model were in (*i*) network topology, (*ii*) method used to generate axon conduction delays between cells, and (*iii*) unitary synaptic conductances.

Network topology. Rather than using a model with five discrete groups of cells, we sought to use a more realistic connectivity. We constructed two overlying arrays, each 30 × 20, of pyramidal cells and interneurons, respectively. This was intended to represent the entire CA1 region (of course, not with realistic numbers of neurons). The lattice spacing in the array is taken to be 150 μm, so that the array is about 6 × 4 mm. Cells are "wired up," so that each neuron receives 50 excitatory inputs, coming from a 5 × 10 band of pyramidal cells overlying the neuron; and it receives 49 inhibitory inputs, coming from a 7 × 7 square of interneurons overlying the cell. The input patterns were the same for pyramidal cells and interneurons. Next, a "slice" was cut, consisting of the lower 6 × 20 part of the array. The resulting 120 pyramidal cells and 120 interneurons were used for the simulations. Note that this network is "distributed" in the sense that cells at the two ends can only communicate with each other via synaptically intercalated interneurons.

Axon conduction delays. Axon conduction delays in the model were calculated from the Euclidean distance between pre- and postsynaptic cells, by assuming a conduction velocity of 0.2 m/s, for axons of pyramidal cells and of interneurons.

Unitary synaptic conductances. As each neuron now has more presynaptic neurons than in previous models, we used somewhat smaller unitary synaptic conductances. With units of nS for conductance and ms for t = time, the unitary conductances were as follows: $e \rightarrow i$, $4 \times t \times \exp(-t/2)$; $i \rightarrow e$, $1.3 \times \exp(-t/10)$; $i \rightarrow i$, $0.5 \times \exp(-t/10)$. Only α-amino-3-hydroxy-5-methyl-4-isoxazolepropionic acid (AMPA) and $GABA_A$-receptor-mediated conductances were simulated.

We verified that this larger model would replicate basic results of the previous model, most importantly that nearly uniform depolarizing conductances delivered to the pyramidal cells and interneurons could lead to gamma-frequency oscillations and that the oscillations were synchronized across the array (to within about 1 ms) under conditions when interneurons fired doublets but not otherwise (13, 19).

RESULTS

Paired tetanic stimuli delivered to two spatially separate areas of CA1 (Fig. 1*a*) generated a posttetanic field oscillation in each area. Each field oscillation consisted of a train of population spikes lasting 2.1 ± 0.1 s, with an initial frequency of 52 ± 2 Hz (Fig. 1*bi*). During the initial 200–400 ms of the oscillation, this frequency was quite stable, as reported previously, and cross-correlation analysis of the two oscillating areas revealed synchrony, with phase lag/lead between the population spikes at each site being <2 ms (1.0 ± 0.6 ms).

Bath application of morphine caused a concentration-dependent disruption of the pattern of oscillation at each site (Fig. 1 *bii* and *biii*). At a concentration of 20–50 μM, a slight increase in population spike frequency was seen at each site and the oscillations decayed over time to reveal small-amplitude field oscillations at about 80 Hz (Fig. 1*bii*, asterisk). Autocorrelation analyses revealed split peaks indicative of a disruption in rhythmicity at each site (Fig. 1*bii*). Cross-correlation analyses of the oscillations at the two sites showed a fixed phase lag/lead and the presence of additional peaks other than those indicative of the fundamental frequency of the oscillation. The phase lag/lead varied markedly from one oscillation to the next but revealed a significant divergence from the synchrony seen in controls (phase lag = 4.6 ± 0.7 ms, $P < 0.05$ compared with controls).

Higher concentrations of morphine (100–200 μM) caused a decrease in the number of observed population spikes in an oscillation and further increased the prevalence of small amplitude high-frequency oscillations (Fig. 1*biii*). These changes were accompanied by a significant decrease in the overall duration of the posttetanic oscillation (control, 2.1 ± 0.1 s; 100 μM morphine, 1.7 ± 0.1 s; $P < 0.05$). Autocorrelation analyses revealed multiple small peaks at one or both sites. Cross-correlations showed the continued presence of a phase lag/lead and a clear diminution of the rhythmicity of the combined two-site oscillation. Addition of 10–20 μM cyprodime, a μ receptor antagonist, to the bathing medium

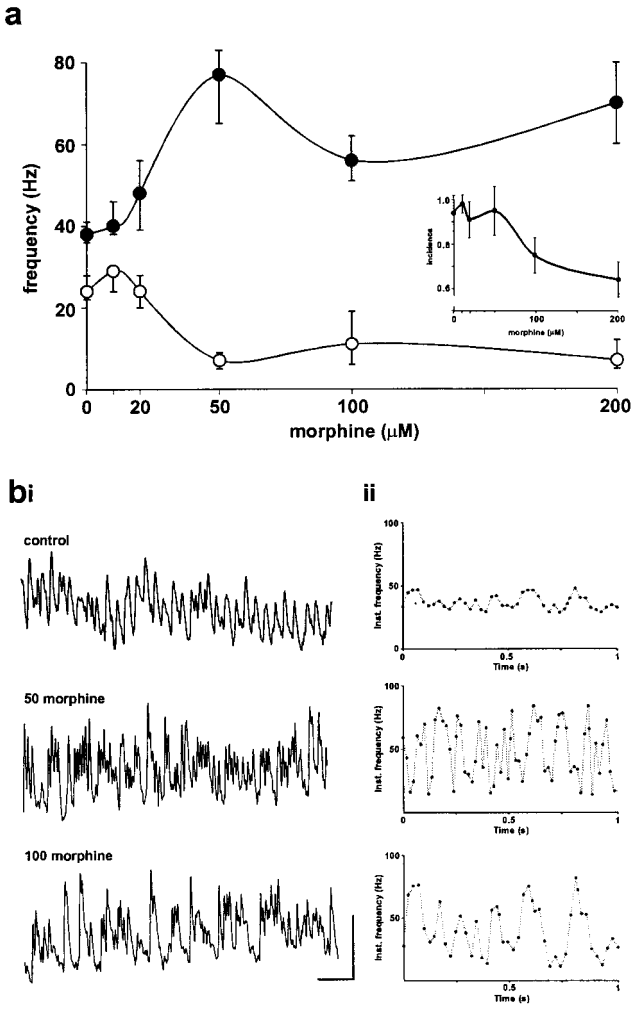

FIG. 2. Morphine disrupts gamma oscillations in pharmacologically isolated interneuron networks. (*a*) Oscillations consisting of pharmacologically isolated $GABA_A$-receptor-mediated synaptic events are detrimentally affected by morphine in a concentration-dependent manner. Isolated inhibitory oscillations ranged from 20 to 40 Hz during activation of metabotropic glutamate receptors in control slices. ●, Maximum frequency during an oscillation; ○, minimum frequency during a train. Morphine (>20 μM) generated a far more erratic pattern of IPSC frequencies with the range increasing almost 4-fold (to 10–80 Hz). (*Inset*) At concentrations above 50 μM, a small but significant decrease in the incidence of evoked oscillations was also seen ($P < 0.05$, control vs. 100 or 200 μM morphine). Trains of IPSCs were analyzed as described in ref 14. (*b*) Examples of individual trains of IPSCs demonstrating the marked increase in maximum frequency and the presence of quiescent periods within an evoked train. Instantaneous frequencies were calculated as $1/(t_{\mathrm{IPSC}_n} - t_{\mathrm{IPSC}_{n-1}})$. Scale bars are 0.5 nA and 100 ms.

Table 1. Effects of morphine on fast inhibitory oscillations are mediated by μ-opioid receptors

Parameter	Control	Morphine (100 μM)	Morphine + cyp	Morphine + nal	Morphine + nor-BNI
Maximum frequency, Hz	38 (36–41)	77 (65–84)*	42 (38–50)†	84 (69–85)	72 (68–90)
Amplitude, nA	0.22 (0.19–0.26)	0.09 (0.06–0.14)*	0.18 (0.16–0.22)†	0.07 (0.06–0.12)	0.10 (0.08–0.15)
τ_D, ms	11 (10–12)	10 (9–11)	10 (9–12)	11 (10–12)	10 (9–10)

The following opiate antagonists were used to verify the effects of morphine on μ-opioid receptors: cyp, cyprodime [(−)-*N*-(cyclopropylmethyl)-4,14-dimethoxymorphinan-6-one, μ receptor, 1–10 μM], nal, naltrindole [17-(cyclopropylmethyl)-6,7-dehydro-4,5α-epoxy-3,14-dihydroxy-6,7-2′,3′-indolomorphinan, δ receptor, 2–20 μM], nor-BNI, nor-binaltorphimine [17,17′-(dicyclopropylmethyl)-6,6′,7,7′,6,6′-imino-7,7′-binorphinan-3,4′,14,14′-tetrol, κ receptor, 10 μM]. Drugs were added to the perfusion solution to assess their ability to antagonize the effects of 100 μM morphine. Frequency, amplitude, and decay time constant (τ_D) were measured for each IPSC within a rhythmic train observed in pyramidal cells. All IPSC oscillation data are expressed as the median (interquartile range, in parentheses, $n = 4$ to 7 animals). Statistical comparisons were made by using nonparametric analysis of variance where appropriate with a minimum of five replicates per slice and concentration of morphine with or without drug. *, IPSC parameters significantly different between morphine and control groups ($P < 0.05$); †, IPSC parameters significantly different between morphine alone and morphine plus opioid antagonist ($P < 0.05$).

during application of 100 μM morphine restored the synchrony of field oscillations to control levels (Fig. 1*biv*).

The effects of morphine on the pattern of oscillation at each site were all mimicked by β-endorphin at 2 μM (Fig. 1*bv*). The posttetanic responses were characterized by infrequent population spikes and a prevalence of fast small-amplitude field oscillations. Waveform analysis showed that these oscillations had a frequency of about 80 Hz as with morphine application and that the synchrony between sites was similarly disrupted.

We have previously shown that the frequency and pattern of gamma oscillations is tightly controlled by the kinetics of the $GABA_A$-receptor-mediated IPSC (10). We therefore examined the effects of morphine on inhibitory oscillations consisting of trains of IPSCs generated by metabotropic glutamate receptor activation to elucidate a possible mechanism for the field oscillation data. Morphine caused a concentration-dependent increase in the maximum frequency of rhythmic inhibitory oscillations. Morphine also decreased the minimum frequency observed during trains of pharmacologically isolated IPSCs (Fig. 2*a*). A significant increase in maximum frequency was seen for concentrations of morphine greater than 20 μM [control, 38 Hz (range 36–41 Hz); 50 μM morphine, 77 Hz (range 65–84 Hz); $P < 0.05$]. The combined effects on faster and slower frequencies resulted in a large increase in the range of frequencies seen during an IPSC train. In the control situation, frequencies varied from 25 to 40 Hz but with 50 μM morphine in the bath, this range more than quadrupled to 10–80 Hz. These effects on IPSC trains were accompanied by a 2-fold decrease in the amplitude of IPSCs measured in pyramidal cells (Table 1) consistent with the primary action of morphine, via μ-opioid receptors, at inhibitory synaptic terminals in the hippocampus (6). The effects of morphine on rhythmic inhibitory oscillation is clearly illustrated in Fig. 2*b*; a stable gamma oscillation in controls is profoundly disturbed and takes the form of brief periods of very fast oscillations (about 80 Hz) punctuated by much slower trains of IPSCs. For a system that relies on these rhythmic oscillations to generate locally and distally synchronous patterns of principal cell firing, the consequences of the effects of morphine are understandably disastrous.

To establish a link between the effects of morphine on the underlying inhibitory oscillation and the network oscillation involving principal cells, we recorded the firing patterns of both inhibitory and pyramidal cells (Fig. 3). Close correlations between experimental data and data from our computer model of conrnu ammonis were seen for firing patterns of both cell types. In the control situation tetanus-induced rhythmic gamma oscillations in pyramidal cells were accompanied by similar firing patterns in inhibitory cells as documented (13, 19). During the presence of 50 μM morphine, however, the rhythmicity of interneuronal firing was disrupted by the appearance of a pattern of burst-like discharges (Fig. 3*b*). These burst discharges were removed by pressure ejection of the AMPA receptor blocker NBQX to the stratum oriens. The

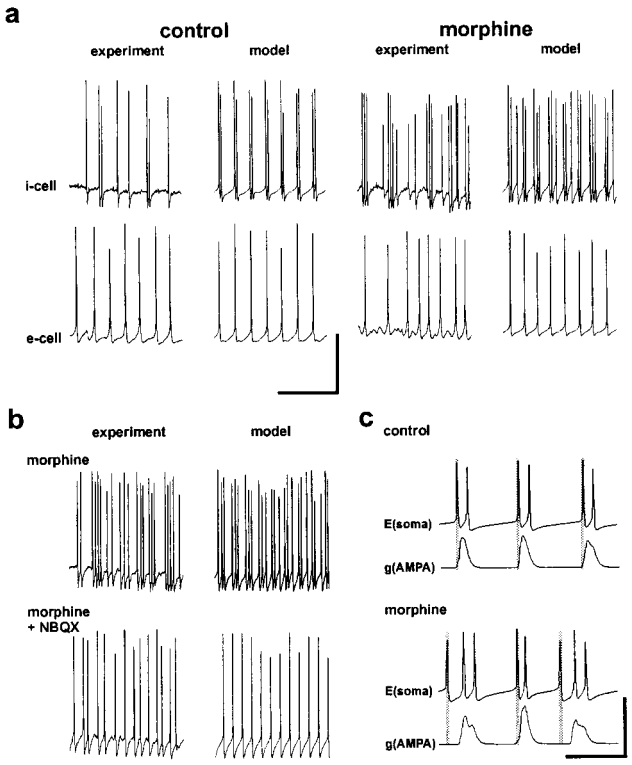

FIG. 3. Morphine-induced burst firing in interneurons through uncoupling of pyramidal cells from the inhibitory rhythm. (*a*) Generation of gamma oscillations at two sites in control conditions results in a rhythmic synchronous firing of action potentials in both inhibitory (i cell) and excitatory (e cell) neurons with cell bodies in stratum pyramidale of area CA1. I cells fire action potential doublets critical for long-range synchrony (see refs. 15 and 19). Experimental recordings were not taken simultaneously from i and e cells, whereas example traces from the model were both taken from one "run." Bath application of morphine (50 μM) disrupts e and i cell firing. In i cells, the normal rhythmic pattern of action potentials is replaced by irregular spiking with "bursts" of action potentials. A very similar pattern of activity is seen in computer simulations simply by reducing the absolute synaptic $GABA_A$ conductance in both e cells and i cells (by 75% and 85% respectively). (*b*) The bursting activity seen in i cells is prevented by bath application or pressure ejection of the AMPA receptor antagonist NBQX (20 μM, $n = 5$). Blockade of AMPA receptors unmasks a faster regular rhythm compared with controls. (*c*) Computer simulations reveal that disconnection of e cells from the i cell inhibitory gamma rhythm (but not vice versa) is responsible for the bursting seen in i cells. In the presence or absence of morphine, the first spike in i cells is generated from the decaying $GABA_A$ IPSC. However, the reduced efficacy of the IPSC in the presence of morphine leads to delayed asynchronous firing of e cells. The resulting excitatory postsynaptic potentials further disrupt i cell firing patterns. Interneuronal IPSCs are also less available to suppress interneuronal bursts. Scale bars are 50 mV and 100 ms (*a* and *b*) and 80 mV/40 nS and 20 ms (*c*).

model shows this observation to be dependent on the degree and form of AMPA-receptor-mediated excitatory postsynaptic potentials (EPSPs) onto inhibitory interneurons (Fig. 3*c*). The multiple mistimed EPSPs causing these bursts were a consequence of reduced synaptic inhibition, (*i*) on pyramidal cells, leading to failure of entrainment and disruption of synchrony, and (*ii*) on interneurons themselves, leading to reduced ability of IPSPs to abort synaptically induced bursts.

DISCUSSION

The present observations demonstrate that morphine and β-endorphin disrupt interneuron network gamma oscillations. Without a coherent rhythmic oscillatory input to projection neurons, the firing pattern of these neurons was also dramatically affected. We have previously demonstrated that for synchronization to take place between two oscillating areas of the archicortex, the output of projection neurons, and specifically their projected synapses onto distal interneurons, must be tightly controlled by the interneuron network (19). Thus failure of inhibitory interneurons to generate a regular gamma rhythm in the presence of morphine elicits a cascade of erroneous timing of both inhibitory and excitatory neuronal firing patterns resulting in the loss of a temporal relationship between two previously synchronous areas.

The observed effects of morphine on the pattern of gamma oscillations and the synchrony between two spatially separate sites were all predicted by the computer model, with the effects of morphine modelled by a decrease in $GABA_A$-receptor-mediated postsynaptic current in both inhibitory and principal cells. The complex firing patterns within the disrupted oscillations appeared as emergent properties of the disinhibited network. In addition, decreasing $GABA_A$ conductances on model interneurons and pyramidal cells led to increased average phase lags between oscillations at separate sites, as in the experiments (see Fig. 1*b*). It was not necessary to model the hyperpolarization of hippocampal inhibitory interneurons produced by μ-opioid receptor activation (8) to predict the above observations. It may be that the strength of the tonic drive generated by the tetanic stimuli (13) is such that the effects of any resting hyperpolarization of inhibitory cells are more than counterbalanced.

That such marked disruption of gamma-induced synchrony could be generated by opiate-mediated disinhibition reinforces the currently held belief that inhibitory oscillations control the timing of principal cell firing patterns. By this mechanism alone, morphine can impede the formation of long-range synchronous discharges in the archicortex. The suspected relationship between these synchronous oscillations and cognitive function indicates that morphine could disturb cognition via disinhibition-induced disruption of interneuron network gamma oscillations. Furthermore, this disruption of long-range synchrony, with relatively less effect locally, also lends weight to the hypothesis that general anesthesia may be caused by a disruption of the functional consequences of "40-Hz" rhythms (12, 22).

We thank A. Bibbig for helpful discussions. This work was supported by the Wellcome Trust and the Human Frontier Science Program. Slice experiments were performed at Imperial College and computer simulations at Birmingham University and the IBM T. J. Watson Research Center. R.D.T. is a Wellcome Principal Research Fellow, H.J.F. holds an Medical Research Council research studentship.

1. Smith, G. M., Semke, C. W. & Beecher, H. K. (1962) *J. Pharmacol. Exp. Ther.* **136,** 53–58.
2. Adams, J. U., Paronis, C. A. & Holtzman, S. G. (1990) *J. Pharmacol. Exp. Ther.* **255,** 1027–1032.
3. Matthes, H. W., Maldonado, R., Simonin, F., Valverde, O., Slowe, S., Kitchen, I., Befort, K., Dierich, A., LeMeur, M., Dolle, P., *et al.* (1996) *Nature (London)* **383,** 819–823.
4. Simon, E. J. & Hiller, J. M. (1978) *Annu. Rev. Pharmacol. Toxicol.* **135,** 371–394.
5. Neumaier, J. F., Mailheau, S. & Chavkin, C. J. (1988) *Pharmacol. Exp. Ther.* **244,** 564–570.
6. Capogna, M., Gähwiler, B. H. & Thompson, S. M. (1993) *J. Physiol.* **470,** 539–558.
7. Kieffer, B. L. (1995) *Cell. Mol. Neurobiol.* **15,** 615–635.
8. Madison, D. V. & Nicoll, R. A. (1988) *J. Physiol.* **398,** 123–130.
9. Whittington, M. A., Traub, R. D. & Jefferys, J. G. R. (1995) *Nature (London)* **373,** 612–615.
10. Traub, R. D., Whittington, M. A., Colling, S. B., Buzsáki, G. & Jefferys, J. G. R. (1996) *J. Physiol.* **493,** 471–484.
11. Llinás, R. R., Grace, A. A. & Yarom, Y. (1991) *Proc. Natl. Acad. Sci. USA* **88,** 897–901.
12. Whittington, M. A., Jefferys, J. G. R. & Traub, R. D. (1996) *Br. J. Pharmacol.* **118,** 1977–1986.
13. Whittington, M. A., Stanford, I. M., Colling, S. B., Jefferys, J. G. R. & Traub, R. D. (1997) *J. Physiol.* **502,** 591–607.
14. Eckhorn, R. (1994) *Prog. Brain Res.* **102,** 405–426.
15. Eckhorn, R., Bauer, R., Jordan, W., Brosch, M., Kruse, W., Munk, M. & Reitboeck, H. J. (1988) *Biol. Cybern.* **60,** 121–130.
16. Singer, W. & Gray, C. M. (1995) *Annu. Rev. Neurosci.* **18,** 555–556.
17. Bragin, A. Jando, G., Nadasdy, Z., Hetke, J., Wise, K. & Buzsáki, G. (1995) *J. Neurosci.* **15,** 47–60.
18. Soltesz, I. & Deschênes, M. (1993) *J. Neurophysiol.* **70,** 97–116.
19. Traub, R. D., Whittington, M. A., Stanford, I. M. & Jefferys, J. G. R. (1996) *Nature (London)* **383,** 621–624.
20. Traub, R. D., Jefferys, J. G. R., Miles, R., Whittington, M. A. & Tóth, K. (1994) *J. Physiol.* **481,** 79–95.
21. Traub, R. D. & Miles, R. (1995) *J. Comput. Neurosci.* **2,** 291–298.
22. Kulli, J. & Koch, C. (1991) *Trends Neurosci.* **14,** 6–10.